Eur. Phys. J. C 17, 279–284 (2000)
Digital Object Identifier (DOI) 10.1007/s100520000454

THE EUROPEAN
PHYSICAL JOURNAL C
© Società Italiana di Fisica
Springer-Verlag 2000

Production of CP-even and CP-odd Higgs bosons at muon colliders

E. Asakawa[1], A. Sugamoto[1], I. Watanabe[2]

[1] Department of Physics and Graduate School of Humanities and Sciences, Ochanomizu University, Tokyo 112-8610, Japan
[2] Akita Keizaihoka University, Akita 010-8515, Japan

Received: 2 April 2000 / Published online: 31 August 2000 – © Springer-Verlag 2000

Abstract. In the s-channel Higgs-boson exchange processes, the interference between the amplitudes for CP-even and CP-odd Higgs bosons is sizable, if the helicities of the initial and final particles are properly fixed and if the mass difference between these bosons is not much larger than their decay widths. We discuss this interference effect in the process $\mu^+\mu^- \to t\bar{t}$. Examining the effect gives us information on the CP-parity for the Higgs bosons and on the sign of the product of the coupling constants for the $H\mu^-\mu^+$, $Ht\bar{t}$, $A\mu^-\mu^+$ and $At\bar{t}$ vertices. The feasibility of observing the interference effect in future muon colliders is evaluated in the framework of the minimal supersymmetric extension of the standard model as an example.

1 Introduction

The standard model (SM) of particle physics predicts one physical neutral CP-even Higgs boson. It can be extended by increasing the number of Higgs fields. In models with more than one Higgs doublet there are two neutral and two charged physical Higgs bosons extra for each additional doublet. If CP is a good symmetry, one neutral boson is CP-even (H) and the other is CP-odd (A). Searches for the Higgs bosons and precise measurements of their properties are indispensable for understanding the mechanism of electroweak symmetry breaking and knowing which model is realized in nature.

A muon collider is an ideal machine to look for the Higgs bosons [1,2], because $\mu^+\mu^-$ pairs are directly annihilated into H and A bosons. The muon beams can be polarized [3]. The feasibility of detecting the Higgs bosons and measuring their properties, such as the masses, total widths and decay branching fractions has been studied in [1,2,4–7]. These references covered the special cases where the H and A bosons are distributed with their resonances overlapping [1] as often expected in the minimal supersymmetric extension of the SM (MSSM), and where mixing between the H and A bosons occurs due to loop-induced CP violation [5]. Moreover, determining the CP nature of the Higgs bosons has also been discussed by using the initial muon polarizations [6].

We here take into consideration overlapping resonances, especially concentrating on interference between the resonances. As was pointed out recently in [8] where the process $\gamma\gamma \to t\bar{t}$ is studied, the amplitudes of s-channel exchanges for the H and A bosons can sizably interfere, if the helicities of the initial and final particles are fixed properly and if the mass difference between these Higgs bosons is at most of the same order as their decay widths. This interference effect disappears if the helicities of both initial and final particles are not fixed. Similar effects are also expected in the process $\mu^+\mu^- \to t\bar{t}$.

In this paper, we discuss the interference effects on the cross section of the process $\mu^+\mu^- \to t\bar{t}$ assuming definite helicities of the initial and final particles. Although the process $\mu^+\mu^- \to t\bar{t}$ is also generated by s-channel γ- and Z-exchange diagrams, their contributions are small under the helicity combinations which induce the s-channel H- and A-exchange amplitudes. The interference effects are measured by the difference between the cross sections for various helicity selections. We estimate the asymmetry between these cross sections. Examining the effects gives us information on the CP-parity for the Higgs bosons. In addition, the asymmetry provides information about the sign of the product of the coupling constants for the $H\mu^-\mu^+$, $Ht\bar{t}$, $A\mu^-\mu^+$ and $At\bar{t}$ vertices. Since this sign depends on the model, we can make judgements of the type of model from the viewpoint of the coupling constants. An example is given in the MSSM which contains two Higgs doublets.

This paper is organized as follows. In Sect. 2 we obtain helicity amplitudes of the process $\mu^+\mu^- \to t\bar{t}$. In Sect. 3 interference effects are discussed and the asymmetry between the cross sections is defined. In Sect. 4 numerical estimates of the cross sections and the asymmetry are given. The degree of polarization of muon beams and a method of helicity observation of the final top pairs are also considered. We give our conclusions in the last section.

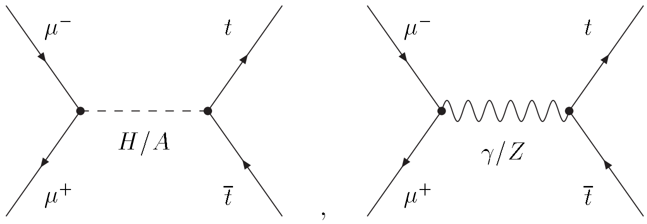

Fig. 1. The diagrams of the process $\mu^+\mu^- \to t\bar{t}$ around the mass poles of the H and A bosons

2 Helicity amplitudes

The process $\mu^+\mu^- \to t\bar{t}$ receives contributions from the diagrams in which H, A, γ and Z are exchanged as shown in Fig. 1. We express the helicity amplitudes for these diagrams as

$$\mathcal{M}_H^{\Lambda\bar{\Lambda}\lambda\bar{\lambda}}, \mathcal{M}_A^{\Lambda\bar{\Lambda}\lambda\bar{\lambda}}, \mathcal{M}_\gamma^{\Lambda\bar{\Lambda}\lambda\bar{\lambda}}, \mathcal{M}_Z^{\Lambda\bar{\Lambda}\lambda\bar{\lambda}}. \tag{2.1}$$

The superscripts Λ and $\bar{\Lambda}$ denote the initial μ^- and μ^+ helicities, while λ and $\bar{\lambda}$ denote the final t and $\bar{t}$ helicities in the center-of-mass frame. Defining λ_i, λ_f as $\Lambda - \bar{\Lambda}$, $\lambda - \bar{\lambda}$, respectively, the amplitudes are given by

$$\mathcal{M}_H^{\Lambda\bar{\Lambda}\lambda\bar{\lambda}} = -4\Lambda\lambda a_\mu a_t g^2 \times \frac{m_\mu m_t}{m_W^2}\beta_\mu\beta_t \frac{s}{s - m_H^2 + i m_H \Gamma_H}\delta_{\lambda_i 0}\delta_{\lambda_f 0}, \tag{2.2}$$

$$\mathcal{M}_A^{\Lambda\bar{\Lambda}\lambda\bar{\lambda}} = -b_\mu b_t g^2 \frac{m_\mu m_t}{m_W^2}\frac{s}{s - m_A^2 + i m_A \Gamma_A}\delta_{\lambda_i 0}\delta_{\lambda_f 0}, \tag{2.3}$$

$$\mathcal{M}_\gamma^{\Lambda\bar{\Lambda}\lambda\bar{\lambda}} = \bar{\Lambda}\bar{\lambda}\frac{16}{3}\pi\alpha_{\rm QED} K_\mu K_t d^1_{\lambda_i\lambda_f}, \tag{2.4}$$

$$\mathcal{M}_Z^{\Lambda\bar{\Lambda}\lambda\bar{\lambda}} = \frac{\pi\alpha_{\rm QED}}{2\sin^2\theta_W\cos^2\theta_W}K_\mu K_t \times \left[F_0\delta_{\lambda_i 0}\delta_{\lambda_f 0} - \bar{\Lambda}\bar{\lambda}F_\mu F_t d^1_{\lambda_i\lambda_f}\right]\frac{s}{s - m_Z^2}, \tag{2.5}$$

$$K_\mu = \delta_{\lambda_i 0}\sqrt{\frac{2}{s}}m_\mu + |\lambda_i|,$$
$$K_t = \delta_{\lambda_f 0}\sqrt{\frac{2}{s}}m_t + |\lambda_f|, \tag{2.6}$$

$$F_0 = \frac{s - m_Z^2}{m_Z^2},$$
$$F_\mu = -1 + 4\sin^2\theta_W + \lambda_i\beta_\mu,$$
$$F_t = +1 - \frac{8}{3}\sin^2\theta_W - \lambda_f\beta_t, \tag{2.7}$$

where g is the weak coupling constant, m_μ, m_t, m_W and m_Z are the masses of muon, top quark, W boson and Z boson; β_t and β_μ are the velocities of the top quarks and the muons in the center-of-mass frame, s is the collision energy squared, and d is the Wigner d function. The masses and the total decay widths of the Higgs bosons are denoted by $m_{H,A}$ and $\Gamma_{H,A}$. The coefficients a_μ, a_t, b_μ and b_t are the coupling constants for $H\mu^-\mu^+$, $Ht\bar{t}$, $A\mu^-\mu^+$ and $At\bar{t}$ vertices, respectively. In the framework of the MSSM, they are expressed as

Table 1. The helicity dependence of the Higgs amplitudes of $\mu^+\mu^- \to H/A \to t\bar{t}$. We denote $\mathcal{M}_{H/A}^{\rm RRRR}$ as $\mathcal{M}_{H/A}$ for simplicity

	$t_{\rm L}\bar{t}_{\rm L}$	$t_{\rm R}\bar{t}_{\rm R}$
$\mu_{\rm L}^-\mu_{\rm L}^+$	$\mathcal{M}_H$	$-\mathcal{M}_H$
	$\mathcal{M}_A$	$\mathcal{M}_A$
$\mu_{\rm R}^-\mu_{\rm R}^+$	$-\mathcal{M}_H$	$\mathcal{M}_H$
	$\mathcal{M}_A$	$\mathcal{M}_A$

$$a_\mu = -\frac{1}{2}\frac{\cos\alpha}{\cos\beta}, \quad a_t = -\frac{1}{2}\frac{\sin\alpha}{\sin\beta},$$
$$b_\mu = \frac{1}{2}\tan\beta, \quad b_t = \frac{1}{2}\cot\beta. \tag{2.8}$$

Here α is the mixing angle of the two CP-even Higgs bosons and $\tan\beta$ is the ratio of the vacuum expectation values of the two Higgs doublets. Here $-4a_\mu a_t$ is almost unity within an accuracy of 13% for $\tan\beta = 1$–100 in the MSSM, which is comparable with $4b_\mu b_t = 1$.

The Higgs-exchange diagrams can contribute only for $\lambda_i = \lambda_f = 0$. The absolute values of $\mathcal{M}_\gamma$ and $\mathcal{M}_Z$ in this case are proportional to m_μ, and negligibly small around the mass poles of the Higgs bosons if the masses of the Higgs bosons are far above m_Z, as will be seen in Sect. 4.2.

3 Interference effects

The signs of the Higgs-exchange amplitudes change under the CP transformation. Expressing $\mathcal{M}_{H,A}^{\rm RRRR}$ as $\mathcal{M}_{H,A}$, where R (L) means the helicity $+1/2$ ($-1/2$), the helicity dependence of the Higgs-exchange amplitudes is summarized in Table 1. With $|{\rm RR}\rangle$ and $|{\rm LL}\rangle$ being spin-zero states of the $t_{\rm R}\bar{t}_{\rm R}$ or the $\mu_{\rm R}^+\mu_{\rm R}^-$, and the $t_{\rm L}\bar{t}_{\rm L}$ or the $\mu_{\rm L}^+\mu_{\rm L}^-$ system, respectively, these states are interchanged under the CP transformation,

$$\mathcal{CP}|{\rm RR}\rangle = -|{\rm LL}\rangle,$$
$$\mathcal{CP}|{\rm LL}\rangle = -|{\rm RR}\rangle. \tag{3.1}$$

For example, $\mathcal{M}_H^{\rm RRRR}$ and $\mathcal{M}_H^{\rm RRLL}$ are related by a CP transformation of the final $t\bar{t}$ system and have the same absolute value of the amplitudes with different signs. As for $\mathcal{M}_A$, the odd contribution of a CP transformation for the final $t\bar{t}$ state is cancelled by the transformation of the CP-odd Higgs boson.

With the helicities fixed, the interference term of the amplitudes for the Higgs bosons, $\Delta\sigma^{\Lambda\bar{\Lambda}\lambda\bar{\lambda}}$, is given by

$$\Delta\sigma^{\Lambda\bar{\Lambda}\lambda\bar{\lambda}} = \frac{N_c}{8\pi s}\frac{\beta_t}{\beta_\mu}\mathcal{R}e[\mathcal{M}_{\phi_1}^{\Lambda\bar{\Lambda}\lambda\bar{\lambda}} \cdot \mathcal{M}_{\phi_2}^{*\Lambda\bar{\Lambda}\lambda\bar{\lambda}}], \tag{3.2}$$

where N_c is the color factor of the top quark; ϕ_1 and ϕ_2 denote the relevant two Higgs bosons. The interference between the amplitudes for two Higgs bosons is manifestly dependent on the relative CP-parity of the Higgs bosons. According to Table 1, the terms $\Delta\sigma^{\Lambda\bar{\Lambda}\lambda\bar{\lambda}}$ for the different helicity states are related to each other. For $\phi_1 = H$ and $\phi_2 = A$,

$$\Delta\sigma^{\mathrm{RRRR}} = \Delta\sigma^{\mathrm{LLLL}} = -\Delta\sigma^{\mathrm{RRLL}} = -\Delta\sigma^{\mathrm{LLRR}}, \quad (3.3)$$

while for $\phi_1 = \phi_2 = H$ or $\phi_1 = \phi_2 = A$

$$\Delta\sigma^{\mathrm{RRRR}} = \Delta\sigma^{\mathrm{LLLL}} = \Delta\sigma^{\mathrm{RRLL}} = \Delta\sigma^{\mathrm{LLRR}}. \quad (3.4)$$

Therefore, a comparison of the interference terms between the different helicity states could provide useful information on the Higgs CP-parity.

As an index for the interference term between two Higgs bosons, we define the asymmetry of the cross sections as

$$\mathcal{A} \equiv \frac{\sigma^{\mathrm{RRRR}} + \sigma^{\mathrm{LLLL}} - \sigma^{\mathrm{RRLL}} - \sigma^{\mathrm{LLRR}}}{\sigma^{\mathrm{RRRR}} + \sigma^{\mathrm{LLLL}} + \sigma^{\mathrm{RRLL}} + \sigma^{\mathrm{LLRR}}}, \quad (3.5)$$

where $\sigma^{\Lambda\overline{\Lambda}\lambda\overline{\lambda}}$ denotes the cross section of $\mu^+\mu^- \to t\bar{t}$ with fixed helicities, which is given by

$$\sigma^{\Lambda\overline{\Lambda}\lambda\overline{\lambda}} = \frac{N_c}{32\pi s}\frac{\beta_t}{\beta_\mu}\int_{-1}^{+1} \mathrm{d}\cos\theta \, |\mathcal{M}^{\Lambda\overline{\Lambda}\lambda\overline{\lambda}}|^2, \quad (3.6)$$

with $\mathcal{M}^{\Lambda\overline{\Lambda}\lambda\overline{\lambda}}$ denoting the sum of the relevant amplitudes, and θ is the scattering angle of the top quarks in the center-of-mass frame. If the cross section receives contributions dominantly from the diagrams mediated by the two Higgs bosons, the cross section can be written as

$$\sigma^{\Lambda\overline{\Lambda}\lambda\overline{\lambda}} = \frac{N_c}{16\pi s}\frac{\beta_t}{\beta_\mu}\{|\mathcal{M}_{\phi_1}|^2 + |\mathcal{M}_{\phi_2}|^2\} + \Delta\sigma^{\Lambda\overline{\Lambda}\lambda\overline{\lambda}}, \quad (3.7)$$

and the asymmetry becomes

$$\mathcal{A} = \frac{2\mathcal{R}e[\mathcal{M}_H \cdot \mathcal{M}_A^*]}{|\mathcal{M}_H|^2 + |\mathcal{M}_A|^2} \quad (\phi_1 = H \text{ and } \phi_2 = A),$$
$$= 0 \quad (\phi_1 = \phi_2 = H \text{ or } \phi_1 = \phi_2 = A). \quad (3.8)$$

Therefore, the observation of a non-vanishing value for $\mathcal{A}$ indicates that the two Higgs bosons have different CP-parities.

In addition, from the sign of $\mathcal{A}$, we can also learn the sign of the product of the coupling constants for $H\mu^-\mu^+$, $Ht\bar{t}$, $A\mu^-\mu^+$ and $At\bar{t}$ vertices. From (2.2) and (2.3),

$$\mathcal{R}e[\mathcal{M}_H \cdot \mathcal{M}_A^*]$$
$$= (a_\mu \cdot a_t \cdot b_\mu \cdot b_t)\beta_\mu\beta_t \, g^4 \, \frac{m_\mu^2 m_t^2}{m_W^4} s^2 \mathcal{D} \quad (3.9)$$

where

$$\mathcal{D} \equiv \frac{(s - m_H^2)(s - m_A^2) + m_H m_A \Gamma_H \Gamma_A}{[(s - m_H^2)^2 + m_H^2\Gamma_H^2][(s - m_A^2)^2 + m_A^2\Gamma_A^2]}. \quad (3.10)$$

The sign of $\mathcal{A}$ is coincident with the sign of $(a_\mu \cdot a_t \cdot b_\mu \cdot b_t)$ in the region of $\mathcal{D} \geq 0$ and is opposite in the region of $\mathcal{D} < 0$.

Table 2. The masses, the total decay widths, the $\mu^+\mu^-$ decay branching ratios and the $t\bar{t}$ decay branching ratios of the H and A bosons in the MSSM adopted in our numerical simulations

$\tan\beta$	m_H (GeV)	Γ_H (GeV)	$\mathrm{Br}(H \to \mu^-\mu^+)$ 10^{-4}	$\mathrm{Br}(H \to t\bar{t})$ 10^{-2}
3.0	403.78	0.79	0.33	74.2
7.0	400.71	0.50	2.84	20.7
15.0	399.97	1.70	3.88	1.30
30.0	399.49	6.67	3.95	0.078
$\tan\beta$	m_A (GeV)	Γ_A (GeV)	$\mathrm{Br}(A \to \mu^-\mu^+)$ 10^{-4}	$\mathrm{Br}(A \to t\bar{t})$ 10^{-2}
3.0	400.00	1.75	0.15	94.6
7.0	400.00	0.67	2.13	45.2
15.0	400.00	1.74	3.80	3.83
30.0	400.00	6.69	3.95	0.25

4 Numerical estimates

4.1 Interference effect in MSSM

Assuming the MSSM as an example for various multi-Higgs doublet models, we present numerical estimates of the asymmetry $\mathcal{A}$. The MSSM includes three neutral Higgs bosons, two of which are CP-even, and the other is CP-odd. The Higgs sector can be parameterized by two parameters, the mass of the CP-odd Higgs boson m_A and the ratio of the vacuum expectation values $\tan\beta$. If m_A is sufficiently large, the mass of the heavier CP-even Higgs boson m_H becomes approximately degenerated into m_A. For definiteness, we take $m_A = 400\,\mathrm{GeV}$ and $\tan\beta = 3$, 7, 15 and 30. The masses, the decay widths and the decay branching ratios of the Higgs bosons from which we derive the coupling constants among Higgs and fermions are computed by the program HDECAY [9], which are listed in Table 2. For the input parameters in the program, the sfermion mass scale is set to $m_{\mathrm{SUSY}} = 1\,\mathrm{TeV}$, the SU(2) gaugino mass parameter M_2 to 500 GeV and the higgsino mixing mass parameter μ to $-500\,\mathrm{GeV}$; this results in heavy supersymmetric particles. No new particles other than Higgs bosons are produced by the decay of the H and A bosons for these parameters.

In Fig. 2 we show the center-of-mass energy dependence of the cross sections for the helicity combinations satisfying $\lambda_i = \lambda_f = 0$. The cross sections for $\Lambda = \overline{\Lambda} = \lambda = \overline{\lambda}$, σ^{LLLL} and σ^{RRRR}, are different from those for $\Lambda = \overline{\Lambda} \neq \lambda = \overline{\lambda}$, σ^{LLRR} and σ^{RRLL}. These differences come from the interference effect between the Higgs-exchange amplitudes. The peak cross section is maximized at $\tan\beta \sim 7$, as $\sigma \simeq 4000\,\mathrm{fb}$. The cross section mediated by γ- and Z-exchange diagrams are smaller than 0.01 fb for $\lambda_i = \lambda_f = 0$, and generally negligible in this energy range. A large interference effect can be seen when the mass difference between the H and A bosons is smaller than their widths and two Higgs-exchange amplitudes have comparable magnitudes, as is shown for $\tan\beta = 15$ and 30 in Fig. 2.

The asymmetry $\mathcal{A}$ for the cross sections is given in Table 3 for several values of $s^{1/2}$ at and around the reso-

Table 3. The cross sections and the asymmetries. We denote $\sigma_{H,A}(P,P,c,\bar{c})$ with γ and Z contributions extracted to be $\sigma_{H,A}(c,\bar{c})$, for simplicity, where P and r are assumed to be +0.6 and 0.2, respectively, and c and $\bar{c}$ are F (forward) or B (backward) of the angle cut

$\tan\beta$	$s^{1/2}$ (GeV)	$\sigma^{\rm LLLL}$ (fb)	$\sigma^{\rm LLRR}$ (fb)	$\mathcal{A}$	$\mathcal{A}'$	$\sigma_{H,A}$(B,F) (fb)	$\sigma_{H,A}$(F,B) (fb)	$\mathcal{A}''$
3.0	400.0	484.9	510.4	−0.026	−0.006	347.5	353.5	−0.009
	402.5	213.8	23.66	0.801	0.079	107.4	61.47	0.272
	405.0	24.56	161.5	−0.736	−0.061	48.29	80.69	−0.251
	406.0	3.260	70.60	−0.912	−0.035	17.49	33.31	−0.311
7.0	399.0	152.2	591.2	−0.591	−0.113	209.1	315.4	−0.203
	400.0	2969.1	4071.7	−0.157	−0.049	2347.1	2610.4	−0.053
	400.5	2358.1	1905.0	0.106	0.032	1557.6	1447.3	0.037
	401.5	1.860	684.7	−0.995	−0.183	159.0	321.1	−0.338
15.0	398.0	16.19	184.6	−0.839	−0.074	50.74	91.60	−0.287
	400.0	95.22	1226.1	−0.856	−0.202	329.8	599.9	−0.291
	401.0	42.70	527.7	−0.850	−0.143	142.5	257.4	−0.287
30.0	390.0	0.88	6.39	−0.758	−0.003	1.93	3.37	−0.272
	400.0	8.20	77.76	−0.809	−0.036	21.88	38.49	−0.275
	405.0	2.43	25.80	−0.828	−0.013	7.08	12.44	−0.275

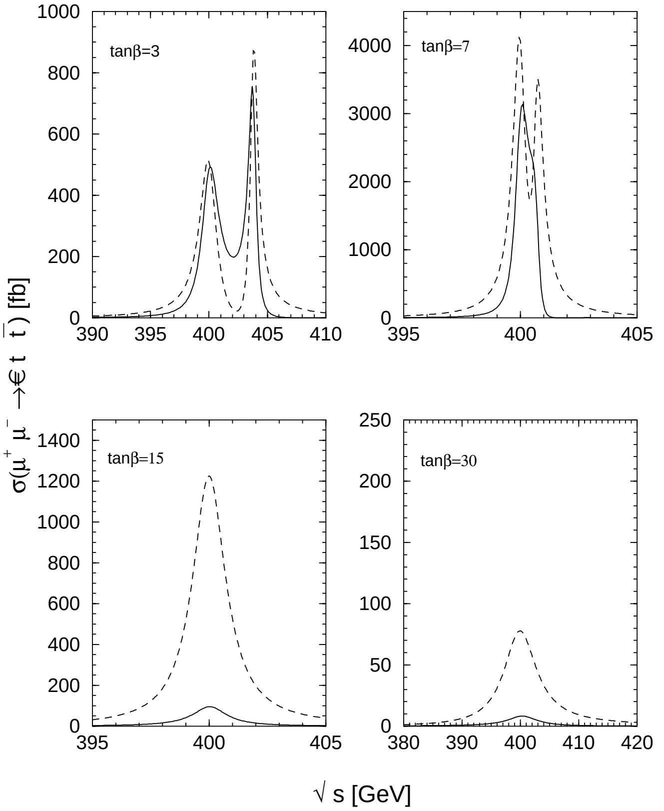

Fig. 2. The cross sections of $\mu^+\mu^- \to t\bar{t}$ with the Higgs resonances for $\tan\beta = 3$, 7, 10 and 30. The solid curves show the cross sections for $\mu^+_{\rm L}\mu^-_{\rm L} \to t_{\rm L}\bar{t}_{\rm L}$ or $\mu^+_{\rm R}\mu^-_{\rm R} \to t_{\rm R}\bar{t}_{\rm R}$, the dashed curves for $\mu^+_{\rm L}\mu^-_{\rm L} \to t_{\rm R}\bar{t}_{\rm R}$ or $\mu^+_{\rm R}\mu^-_{\rm R} \to t_{\rm L}\bar{t}_{\rm L}$

nances. The asymmetry reaches $\mathcal{O}(1)$ in certain ranges of $s^{1/2}$, showing the strong effect of the interference between H and A. Since $\mathcal{A}$ is negative for $s^{1/2} < m_{H,A}$, we can deduce

$$a_\mu \cdot a_t \cdot b_\mu \cdot b_t < 0, \tag{4.1}$$

which is consistent with (2.8).

4.2 Beam polarization and helicity observation

The above arguments did not take account of the degree of polarization of the initial muon beams and the helicity observation of the final top pairs. As was mentioned in Sect. 2, the absolute values of the amplitudes of γ- and Z-exchange diagrams with helicity combinations other than $\lambda_i = \lambda_f = 0$ are generally larger than those with $\lambda_i = \lambda_f = 0$ (Fig. 3). Therefore, the background processes $\mu^+\mu^- \to \gamma/Z \to t\bar{t}$ should be considered as long as the polarization of muon beams and the efficiency of the helicity observation of the top pairs are not perfect. The cross sections are contaminated with these backgrounds.

There are some statistical methods to measure the top-quark helicity [8,10,11]. As an illustration, we follow [8]. The bottom quark decaying from a top quark has an angular distribution proportional to $0.5 - 0.2\lambda\cos\theta$, where θ is the emission angle of the bottom quark in the rest frame of the decaying top quark with respect to the direction of the top momentum in the $t\bar{t}$ c.m. frame. The anti-bottom quark has a distribution proportional to $0.5 + 0.2\bar{\lambda}\cos\bar{\theta}$, where $\bar{\theta}$ is the emission angle of the anti-bottom quark[1]. Therefore, an event with the top quark decaying forward

[1] In order to derive the emission angles, θ and $\bar{\theta}$, one needs to identify the charge and the momentum of the top and the anti-top quarks. These tasks can be done by observing their decay products. For example, when one W decays leptonically and the other decays hadronically, we can generally reconstruct the top and the anti-top decay kinematics. Semileptonic decays of the B mesons can be used when both W's decay hadronically. The efficiency of the analysis of such $t\bar{t}$ reconstructions is discussed in [12]

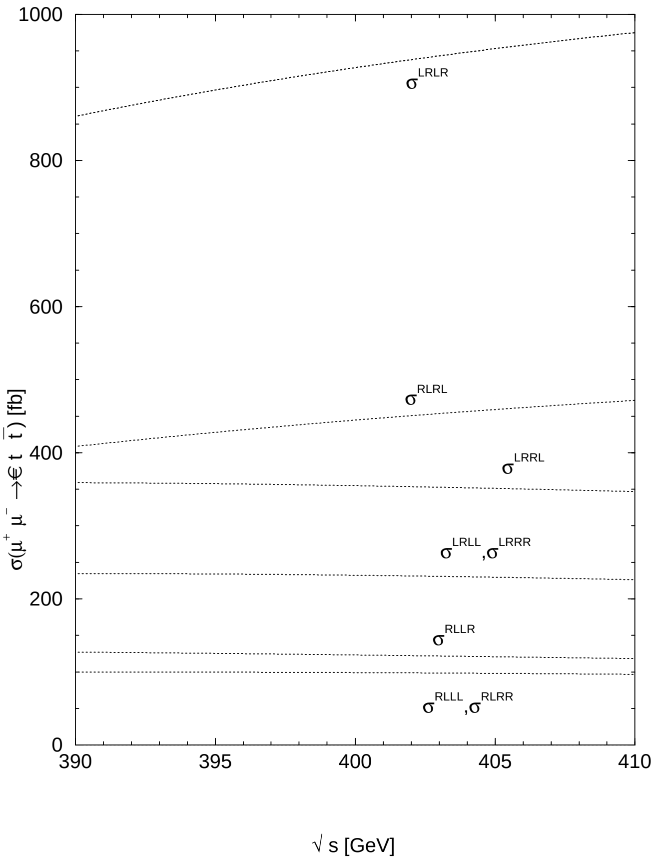

Fig. 3. The cross sections of $\mu^+\mu^- \to \gamma/Z \to t\bar{t}$. The cross sections $\sigma^{\rm LLLL}$, $\sigma^{\rm LLRR}$, $\sigma^{\rm RRRR}$, $\sigma^{\rm RRLL}$, $\sigma^{\rm LLLR}$, $\sigma^{\rm LLRL}$, $\sigma^{\rm RRLR}$ and $\sigma^{\rm RRRL}$ are smaller than 0.01 [fb]

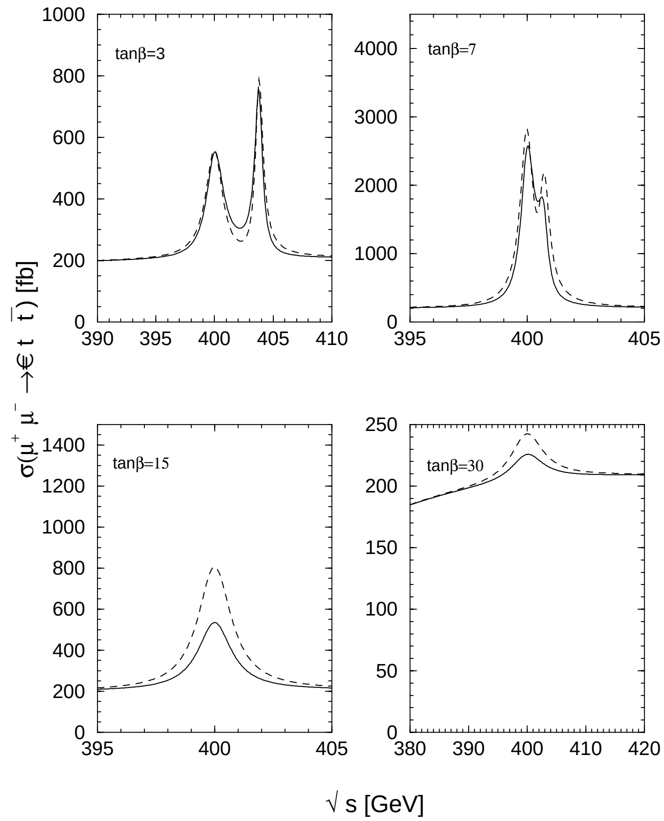

Fig. 4. The effective cross sections of $\mu^+\mu^- \to t\bar{t}$ for $\tan\beta =$ 3, 7, 10 and 30. The solid curves are for $\sigma(P,P,\mathrm{B},\mathrm{F})$ or $\sigma(-P,-P,\mathrm{F},\mathrm{B})$, while the dashed curves are for $\sigma(P,P,\mathrm{F},\mathrm{B})$ or $\sigma(-P,-P,\mathrm{B},\mathrm{F})$, with $P = +0.6$ and $r = 0.2$

and with the anti-top quark decaying backward is most likely to be a $t_{\rm L}\bar{t}_{\rm L}$ event. Applying the emission angle cuts F (forward, $0 < \cos\theta, \cos\overline{\theta} < +1$) and B (backward, $-1 < \cos\theta, \cos\overline{\theta} < 0$) to the bottom quark direction, the counted numbers of polarized top and anti-top decay events are reduced by the factor R and $\overline{R}$, respectively:

$$\begin{aligned} R(\mathrm{F},\lambda) &= \frac{1-2\lambda r}{2},\ R(\mathrm{B},\lambda) = \frac{1+2\lambda r}{2}, \\ \overline{R}(\mathrm{F},\overline{\lambda}) &= \frac{1+2\overline{\lambda} r}{2},\ \overline{R}(\mathrm{B},\overline{\lambda}) = \frac{1-2\overline{\lambda} r}{2}, \end{aligned} \tag{4.2}$$

where r is $r_{\rm B} - r_{\rm F}$ in [8], and its value is estimated to be 0.2 by this method. If one observes the direction of the charged lepton from the $t \to bW \to bl\nu$ decay [11], instead of the bottom quark direction, r reaches 0.5 in the Born approximation.

We define the effective cross sections as follows:

$$\sigma(P_{\mu^-}, P_{\mu^+}, c, \bar{c}) = \sum_{\Lambda\overline{\Lambda}\lambda\overline{\lambda}} \sigma^{\Lambda\overline{\Lambda}\lambda\overline{\lambda}} \frac{(1+2\Lambda P_{\mu^-})}{2} \times \frac{(1+2\overline{\Lambda} P_{\mu^+})}{2} R(c,\lambda)\overline{R}(\bar{c},\overline{\lambda}), \tag{4.3}$$

where P_{μ^-} and P_{μ^+} denote the degrees of polarization of μ^- and μ^+, and c and $\bar{c}$ are F or B, respectively. The effective cross sections are shown in Fig. 4, assuming $|P_{\mu^-}| = |P_{\mu^+}| = 0.6$ as an example. To extract the Higgs signal efficiently, we should select $P_{\mu^-} = P_{\mu^+} = P$ and $c = \mathrm{F}$ and $\bar{c} = \mathrm{B}$ or $c = \mathrm{B}$ and $\bar{c} = \mathrm{F}$. In these selections, the background cross sections of γ and Z are independent on the signs of the P's and the choice of c. There is another interference contribution between the Higgs-exchange and the γ- or Z-exchange amplitude for $\lambda_i = \lambda_f = 0$, and this interference has helicity dependence; however, it is negligibly small. With the polarizations and the emission angle cuts, we can define another asymmetry of the cross sections between the different cuts, with P unchanged.

$$\begin{aligned} \mathcal{A}' &= \frac{\sigma(P,P,\mathrm{B},\mathrm{F}) - \sigma(P,P,\mathrm{F},\mathrm{B})}{\sigma(P,P,\mathrm{B},\mathrm{F}) + \sigma(P,P,\mathrm{F},\mathrm{B})} \\ &= \frac{\sigma^{\rm diff}}{\sigma^{\rm tot}}, \\ \sigma^{\rm diff} &= \frac{\epsilon}{4}\{(1+P)^2(\sigma^{\rm RRRR} - \sigma^{\rm RRLL}) \\ &\quad + (1-P)^2(\sigma^{\rm LLRR} - \sigma^{\rm LLLL})\}, \\ \sigma^{\rm tot} &= \frac{1}{8}\{(1+P)^2[(1+\epsilon^2)(\sigma^{\rm RRRR} + \sigma^{\rm RRLL}) \\ &\quad + (1-\epsilon^2)(\sigma^{\rm RRRL} + \sigma^{\rm RRLR})] \\ &\quad + (1-P^2)[(1+\epsilon^2) \\ &\quad \times (\sigma^{\rm LRRR} + \sigma^{\rm RLLL} + \sigma^{\rm RLRR} + \sigma^{\rm LRLL}) \end{aligned} \tag{4.4}$$

$$+ (1-\epsilon^2)(\sigma^{\mathrm{LRRL}} + \sigma^{\mathrm{RLLR}} + \sigma^{\mathrm{RLRL}} + \sigma^{\mathrm{LRLR}})] + (1-P)^2[(1+\epsilon^2)(\sigma^{\mathrm{LLRR}} + \sigma^{\mathrm{LLLL}}) + (1-\epsilon^2)(\sigma^{\mathrm{LLRL}} + \sigma^{\mathrm{LLLR}})]\}. \quad (4.5)$$

As is demonstrated in Table 3, the ratio of the asymmetries $\mathcal{A}/\mathcal{A}^{'}$ is at least three and sometimes reaches several tens, which means there is a strong suppression due to the γ and Z contributions.

Since the γ- and Z-exchange cross sections are well known, we can define the other asymmetry $\mathcal{A}^{''}$ on extracting the γ and Z contributions:

$$\mathcal{A}^{''} = \frac{\sigma(P,P,\mathrm{B,F}) - \sigma(P,P,\mathrm{F,B}) - \sigma^{\mathrm{diff}}_{\gamma,Z}}{\sigma(P,P,\mathrm{B,F}) + \sigma(P,P,\mathrm{F,B}) - \sigma^{\mathrm{tot}}_{\gamma,Z}}, \quad (4.6)$$

where $\sigma^{\mathrm{diff}}_{\gamma,Z}$ and $\sigma^{\mathrm{tot}}_{\gamma,Z}$ are the γ and Z contributions to σ^{diff} and σ^{tot}, respectively. Here $\sigma^{\mathrm{diff}}_{\gamma,Z}$ is vanishing. Since we have extracted the background effects of the γ- and Z-exchange from $\mathcal{A}^{'}$, $\mathcal{A}^{''}$ is proportional to $\mathcal{A}$:

$$\mathcal{A}^{''} = \frac{4}{\left(\frac{1}{r}+r\right)\left(\frac{1}{P}+P\right)}\mathcal{A}. \quad (4.7)$$

When $\mathcal{A}^{''} > 0.1\mathcal{A}$ is required, $r > 0.3$ for $P = 0.1$ [4], and $P > 0.13$ for $r = 0.2$. The values for $P = 0.6$ and $r = 0.2$ are shown in Table 3.

Neglecting the systematic errors and assuming 100% efficiency, we found that the required luminosity to establish the non-zero asymmetry $\mathcal{A}^{''}$ is least at a moderate value of $\tan\beta$. Only $\gtrsim 20\,\mathrm{pb}^{-1}$ of the integrated luminosity enables us to perceive a non-vanishing asymmetry within 1σ statistical error for $\tan\beta = 15$, and $30\,\mathrm{pb}^{-1}$ for $\tan\beta = 7$. For $\tan\beta = 3$ and 30, $0.25\,\mathrm{fb}^{-1}$ and $1.5\,\mathrm{fb}^{-1}$ are required, respectively.

5 Conclusions

We have discussed the interference effect on the cross section of the process $\mu^+\mu^- \to t\bar{t}$ with the H and A resonances almost degenerated. The interference between the H and A bosons arises if muon beams are longitudinally polarized and if we observe the helicities of the top quarks. The interference effect can be measured by observing the difference between the cross sections with appropriate helicity combinations. It has been shown that the existence of the difference can be reliable evidence of the existence of both H and A bosons, while the absence indicates the existence of only H bosons or A bosons around the resonances. It is especially important that the existence of the H and A bosons can be established even if their masses are degenerated, by observing the interference effect in the overlapping resonances. We have estimated the asymmetry between the cross sections adopting the MSSM as an example. Even after taking into account the background γ- and Z-exchange contributions because of incompleteness of the polarizations of muon beams and the measurement of top-quark helicities, the absolute values of the asymmetry can be detectable in certain ranges of $s^{1/2}$. If we can accumulate the luminosities which enable us to observe the asymmetry, it is possible to learn not only the existence of the H and A bosons but also the sign of the product of the coupling constants of the Higgs bosons to the fermions from the sign of the asymmetry.

Acknowledgements. The authors thank K. Hagiwara and N. Oshimo for valuable discussions and reading the manuscript. They also would like to thank K. Fujii, K. Ikematsu and T. Ohgaki for useful comments. This work is supported in part by the Grant-in-Aid for Scientific Research (No. 11640262) and the Grant-in-Aid for Scientific Research on Priority Areas (No. 11127205) from the Ministry of Education, Science and Culture, Japan.

References

1. V. Barger, M.S. Berger, J.F. Gunion, T. Han, Phys. Rep. **286**, 1 (1997)
2. V. Barger, M.S. Berger, J.F. Gunion, T. Han, Phys. Rev. Lett. **75**, 1462 (1995); B. Kamal, W.J. Marciano, Z. Parsa, in Workshop on Physics at the First Muon Collider and Front End of a Muon Collider, edited by S. Geer, R. Raja, AIP Conference Proceedings 435 p. 657 (hep-ph/9712270)
3. B. Norum, R. Rossmanith, Nucl. Phys. (Proc. Suppl.) B **51a**, 191 (1996)
4. C.M. Ankenbrandt et al., Phys. Rev. ST Accel. Beams **2**, 081001 (1999); V. Barger, M.S. Berger, J.F. Gunion, T. Han, Phys. Rev. Lett. **78**, 3991 (1997); J.F. Gunion, in Proceedings of the 5th International Conference on Physics Beyond the Standard Model, Balholm, Norway, 1997, edited by G. Eigen, P. Osland, B. Stugu (AIP, Woodbury, New York 1997), p. 234 (hep-ph/9707379); V. Barger, T. Han, C.-G. Zhou, hep-ph/0002042
5. A. Pilaftsis, Phys. Rev. Lett. **77**, 4996 (1996); K.S. Babu, C. Kolda, J. March-Russell, F. Wilczek, Phys. Rev. D **59**, 016004 (1999); S.Y. Choi, M. Drees, Phys. Rev. Lett. **81**, 5509 (1998); S.Y. Choi, J.S. Lee, hep-ph/9909315
6. B. Grzadkowski, J.F. Gunion, J. Pliszka, hep-ph/0003091
7. D. Atwood, A. Soni, Phys. Rev. D **52**, 6271 (1995)
8. E. Asakawa, J. Kamoshita, A. Sugamoto, I. Watanabe, Eur. Phys. J. C 14, 335 (2000)
9. A. Djouadi, J. Kalinowski, M. Spira, Comm. Phys. Commun. Res. **108**, 56 (1998)
10. K. Hagiwara, H. Murayama, I. Watanabe, Nucl. Phys. B **367**, 257 (1991)
11. M. Ježabek, J.H. Kühn, Nucl. Phys. B **320**, 20 (1989); G. Mahlon, S. Parke, Phys. Rev. D **53**, 4886 (1996)
12. G.A. Ladinsky, C.-P. Yuan, Phys. Rev. D **49**, 4415 (1994); R. Frey, in Proceedings of the Workshop on Physics and Experiments with Linear Colliders (LCWS95), Iwate, Japan, September, 1995, edited by A. Miyamoto et al. (World Scientific, 1996), p. 144 (hep-ph/9606201); R. Frey et al., hep-ph/9704243, Report of the Top Physics working group at the 1996 DPF/DPB Snowmass workshop